



Contents lists available at ScienceDirect

# Spectrochimica Acta Part A: Molecular and Biomolecular Spectroscopy

journal homepage: [www.elsevier.com/locate/saa](http://www.elsevier.com/locate/saa)

## An experimental and DFT study of a disulfide-linked Schiff base: Synthesis, characterization and crystal structure of bis (3-methoxy-salicylidene-2-aminophenyl) disulfide in its anhydrous and monohydrate forms



Verónica Ferraresi-Curotto<sup>a,b</sup>, Gustavo A. Echeverría<sup>c</sup>, Oscar E. Piro<sup>c</sup>, Reinaldo Pis-Diez<sup>a</sup>, Ana C. González-Baró<sup>a,\*</sup>

<sup>a</sup>CEQUINOR (CONICET, UNLP), CC 962, B1900AVV La Plata, Argentina

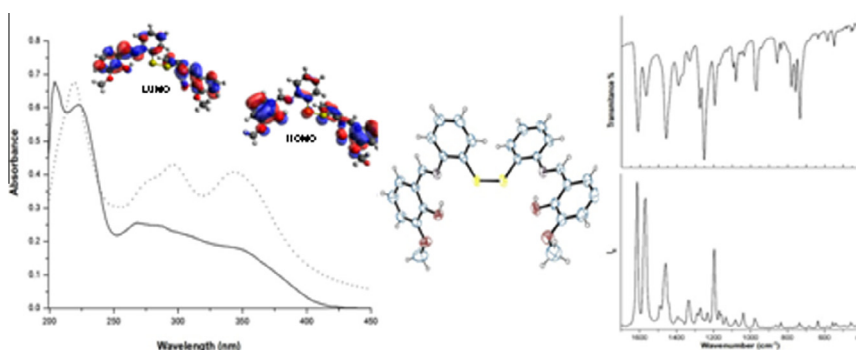
<sup>b</sup>Depto. de Química, FAcEYN-UNCa, Av. Belgrano 300, K4700AAP Catamarca, Argentina

<sup>c</sup>IFLP (CONICET, UNLP), CC 67, B1900AVV La Plata, Argentina

### HIGHLIGHTS

- Disulfide Schiff base from condensation of 2-aminothiophenol and *o*-vanillin.
- X-ray diffraction crystal structures of the anhydrous and monohydrate forms.
- Vibrational and electronic spectra assigned with the help of DFT calculations.

### GRAPHICAL ABSTRACT



### ARTICLE INFO

#### Article history:

Received 18 April 2013

Received in revised form 9 August 2013

Accepted 15 August 2013

Available online 29 August 2013

#### Keywords:

2-Aminothiophenol

*o*-Vanillin

X-ray diffraction

Spectroscopy

DFT calculations

### ABSTRACT

A detailed structural and spectroscopic study of the disulfide Schiff base obtained from condensation of 2-aminothiophenol and *o*-vanillin is reported. It includes the analyses of the anhydrous and monohydrate forms of the title compound. Structures of both solids were resolved by X-ray diffraction methods. A comparison between experimental and theoretical results is presented. The conformational space was searched and geometries were optimized both in gas phase and including solvent effects. Vibrational (IR and Raman) and electronic spectra were measured and assigned with the help of computational methods based on the Density Functional Theory. Calculated MEP-derived atomic charges were calculated to predict coordination sites for metal complexes formation.

© 2013 Elsevier B.V. All rights reserved.

### Introduction

A large number of Schiff bases with ONO and ONS donor groups and their complexes have been extensively studied with the aim of

understanding the role of metals in biological systems [1–4], as well as their interesting properties including antibacterial activity against human pathogenic bacteria [5,6], quelation effect towards certain toxic metals [7–10] and anticancer activity [11]. Also, interesting electrochemical properties of some Schiff bases containing disulfide bonds have been tested in several applications. Compounds of this family showed anti-corrosive effects on mild steel

\* Corresponding author. Tel.: +54 221 4240172.

E-mail address: [agb@quimica.unlp.edu.ar](mailto:agb@quimica.unlp.edu.ar) (A.C. González-Baró).

[12] and others are good candidates for manufacturing organic–inorganic hybrid devices [13]. Some of them behave as redox-active multi-dentate ligands in the electro-catalytic alcohol oxidation potentially useful in methanol fuel cells [14]. In particular, ligands obtained by condensation of 2-aminothiophenol with different aldehydes and ketones and their complexes are a research subject of continuous interest [3,6–11,14–17]. Among these, the products obtained by the reaction between 2-aminothiophenol with salicylaldehyde and some derivatives have been extensively characterized by many authors [4,7–10,15,16,18–20]. One of the derivatives employed in the synthesis is 2-hydroxy-3-methoxybenzaldehyde (3-methoxysalicylaldehyde or, for short, *o*-HVa), an aldehyde with well known properties [20,21].

Here we report a detailed study of the disulfide Schiff base, obtained from condensation of 2-aminothiophenol (hereafter AT, Scheme 1) and *o*-HVa (Scheme 2) in ethanol. The compound, bis (3-methoxy-salicylidene-2-aminophenyl) disulfide, was prepared in two crystal forms, anhydrous and as a monohydrate [hereafter referred to as (HvananS)<sub>2</sub> and (HvananS)<sub>2</sub>·H<sub>2</sub>O; see Scheme 3]. Both crystal structures were determined by X-ray diffraction methods and are presented here along with experimental and theoretical results for (HvananS)<sub>2</sub>. Vibrational (IR and Raman) and electronic spectra were analyzed and assigned with the help of computational methods based on the Density Functional Theory.

## Experimental methods

### Synthesis

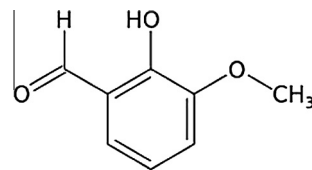
All chemicals were of analytic grade and used as purchased. Melting points were determined using a Bock monoscop “M” instrument.

#### *Anhydrous bis (3-methoxy-salicylidene-2-aminophenyl) disulfide [(HvananS)<sub>2</sub>]*

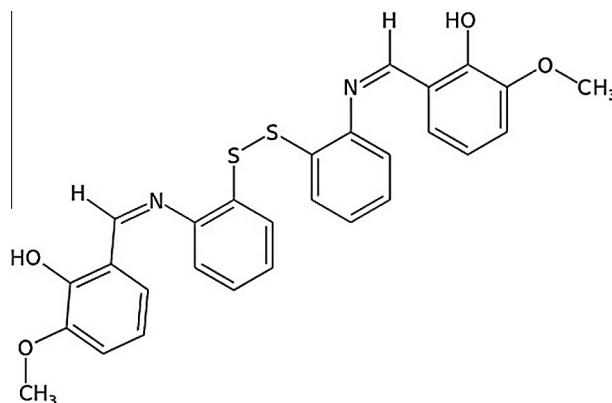
The compound was prepared according to the reported procedure for the condensation reaction of 2-aminothiophenol and salicylaldehyde [8], replacing the aldehyde by *o*-HVa. Twenty milliliters of hot ethanolic solution containing 1 mmol of *o*-HVa (Sigma) was drop-wise added to a solution of 1 mmol of AT (Sigma) in 20 ml of ethanol (Merck), with continuous stirring and mild heating. The starting yellow color solution was refluxed for 2 h before turning orange. After 24 h, orange single crystals suitable for X-ray structural work were formed. They were filtered out, washed with cold ethanol and dried in a desiccator (yield 45%, m.p.: 179–180 °C). This synthesis differs from the one informed by Wang et al. [4] since they used as reactant 2,2'-diaminodiphenyl disulfide instead of AT.

#### *Bis (3-methoxy-salicylidene-2-aminophenyl) disulfide monohydrate [(HvananS)<sub>2</sub>·H<sub>2</sub>O]*

Five milliliters of hot bi-distilled water was drop-wise added to twenty milliliters of an ethanol solution containing 0.05 mmol of (HvananS)<sub>2</sub>, upon continuous stirring and mild heating. The starting pale orange solution was refluxed for 1 h when it turned to an orange-color solution. After five days, orange needle-like single



Scheme 2. Schematic representation of 3-methoxysalicylaldehyde.



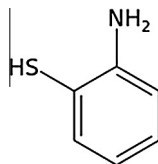
Scheme 3. Schematic representation of the Schiff base (HvananS)<sub>2</sub>.

crystals, suitable for structural X-ray diffraction analysis were formed. They were filtered out, washed with cold ethanol and then stored in a desiccator (yield 68%, m.p.: 168–169 °C).

### X-ray diffraction data

The measurements were performed on an Oxford Xcalibur Gemini, Eos CCD diffractometer with graphite-monochromated Cu K $\alpha$  ( $\lambda = 1.54178$  Å) radiation. X-ray diffraction intensities were collected ( $\omega$  scans with  $\vartheta$  and  $\kappa$ -offsets), integrated and scaled with CrysAlisPro [22] suite of programs. The unit cell parameters were obtained by least-squares refinement (based on the angular settings for all collected reflections with intensities larger than seven times the standard deviation of measurement errors) using CrysAlisPro. Data was corrected empirically for absorption employing the multi-scan method implemented in CrysAlisPro. The structures were solved by direct methods with SHELXS-97 [23] and the molecular models refined by full-matrix least-squares procedure on  $F^2$  with SHELXL-97 [24].

All but the hydroxyl hydrogen atoms were located stereochemically and refined with the riding model. The methyl H-positions were optimized by treating them as rigid groups which were allowed to rotate during the refinement around the corresponding O–C bonds such as to maximize the residual electron density at the calculated H-positions. As a result, all CH<sub>3</sub> groups converged to staggered conformations. The hydroxyl H-atoms were located in a difference Fourier map and refined at their found position with isotropic displacement parameters. Crystal data and structure refinement results are summarized in Table 1.



Scheme 1. Schematic representation of 2-aminothiophenol.

**Table 1**

Crystal data and structure refinement results for bis (3-methoxy-salicylidene-2-aminophenyl) disulfide in both crystal forms.

	Anhydrous	Monohydrate
Empirical formula	C <sub>28</sub> H <sub>24</sub> N <sub>2</sub> O <sub>4</sub> S <sub>2</sub>	C <sub>28</sub> H <sub>26</sub> N <sub>2</sub> O <sub>5</sub> S <sub>2</sub>
Formula weight	516.61	534.63
Temperature (K)	295(2)	297(2)
Wavelength (Å)	1.54184	1.54184
Crystal system	Triclinic	Monoclinic
Space group	P-1	C2/c
<i>Unit cell dimensions</i>		
<i>a</i> (Å)	<i>a</i> = 10.6819(6)	24.816(1)
<i>b</i> (Å)	<i>b</i> = 12.2977(5)	7.3862(4)
<i>c</i> (Å)	<i>c</i> = 19.970(1)	28.331(2)
$\alpha$ (°)	$\alpha$ = 86.436(4)	90.00
$\beta$ (°)	$\beta$ = 88.585(4)	96.916(5)
$\gamma$ (°)	$\gamma$ = 82.399(4)	90.00
Volume (Å <sup>3</sup> )	2594.9(2)	5155.2(5)
<i>Z</i>	4	8
Density (calculated, Mg/m <sup>3</sup> )	1.322	1.378
Absorption coefficient (mm <sup>-1</sup> )	2.163	2.225
F(000)	1080	2240
Crystal shape/color	Fragment/yellow	Prism/yellow
Crystal size (mm <sup>3</sup> )	0.223 × 0.123 × 0.077	0.268 × 0.073 × 0.056
$\theta$ -Range (°) for data collection	3.63–74.04	3.59–71.00
Index ranges	−13 ≤ <i>h</i> ≤ 13, −15 ≤ <i>k</i> ≤ 11, −24 ≤ <i>l</i> ≤ 24	−26 ≤ <i>h</i> ≤ 30, −8 ≤ <i>k</i> ≤ 4, −32 ≤ <i>l</i> ≤ 34
Reflections collected	18773	8664
Independent reflections	10354 [R(int) = 0.0272]	4952 [R(int) = 0.0302]
Observed reflections [ <i>I</i> > 2 $\sigma$ ( <i>I</i> )]	7399	3242
Completeness (%) to $\theta = 74.04^\circ$	98.3	99.5
Absorption correction	Semi-empirical from equivalents	Semi-empirical from equivalents
Max. and min. transmission	1.000 and 0.843	1.000 and 0.851
Refinement method	Full-matrix least-squares on <i>F</i> <sup>2</sup>	Full-matrix least-squares on <i>F</i> <sup>2</sup>
Data/restraints/parameters	10354/0/669	4952/3/344
Goodness-of-fit on <i>F</i> <sup>2</sup>	1.251	1.074
Final <i>R</i> indices <sup>a</sup> [ <i>I</i> > 2 $\sigma$ ( <i>I</i> )]	<i>R</i> <sub>1</sub> = 0.0483, <i>wR</i> <sub>2</sub> = 0.1619	<i>R</i> <sub>1</sub> = 0.0451, <i>wR</i> <sub>2</sub> = 0.1054
<i>R</i> indices (all data)	<i>R</i> <sub>1</sub> = 0.0735, <i>wR</i> <sub>2</sub> = 0.1845	<i>R</i> <sub>1</sub> = 0.0809, <i>wR</i> <sub>2</sub> = 0.1406
Largest diff. peak and hole (e Å <sup>-3</sup> )	0.246 and −0.268	0.204 and −0.272

$$^a R_1 = \frac{\sum ||F_o| - |F_c||}{\sum |F_o|}, wR_2 = \left[ \frac{\sum w(|F_o|^2 - |F_c|^2)^2}{\sum w(|F_o|^2)^2} \right]^{1/2}.$$

### Spectroscopic analysis

FTIR absorption spectra (4000–400 cm<sup>-1</sup>) were measured using the KBr pellet technique with a FTIR Bruker Equinox 55 instrument. Raman dispersion spectra of solid samples were obtained with a Bruker IFS 66 FTIR spectrophotometer, using the FRA 106 Raman accessory and the 1064 nm line of a Nd:YAG solid state laser for excitation. The electronic absorption spectra of (HvananS)<sub>2</sub> was measured on an ethanolic solution (3 × 10<sup>-5</sup> M) in the 200–800 nm spectral range. It was recorded with a Hewlett–Packard 8452-A diode array spectrometer using 10 mm quartz cells.

### Computational methods

The conformational space of (HvananS)<sub>2</sub> was explored with the aid of the semi-empirical PM6 method [25]. Several starting geometries derived from selected variations in the C11–S1–S2–C21, S1–C11–C16–N11, C16–N11–C17–C18, N11–C17–C18–C19, S2–C21–C26–N21, C26–N21–C27–C28 and N21–C27–C28–C29 torsion angles were considered (see Fig. 1 for atom labeling). Geometries obtained from X-ray diffraction were also used as a starting point for the optimizations.

Geometries obtained with the PM6 method were re-optimized using the hybrid PBE0 [26] functional of the Density Functional Theory (DFT) with the triple- $\zeta$  6-311+G(d) basis set [27–29]. The critical points found after optimization were characterized by the sign of the eigenvalues of the Hessian matrix of the total electronic energy with respect to the nuclear coordinates. When the critical point corresponded to a minimum on the potential energy surface of the mole-

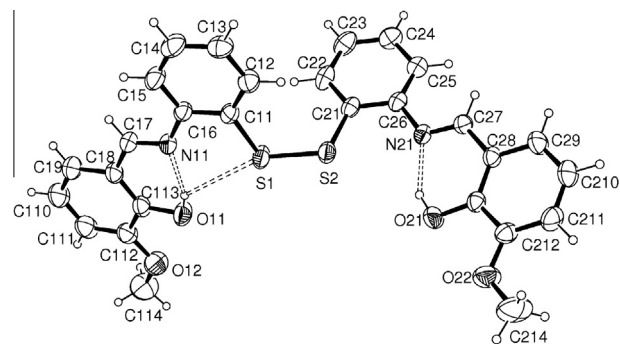


**Fig. 1.** ORTEP drawing of (HvananS)<sub>2</sub> showing the labeling of the non-H atoms and their displacement ellipsoids at the 30% probability level. H-bonds are indicated by dashed lines. For clarity, only one of the independent molecules is depicted.

cule, the eigenvalues were converted to harmonic vibrational frequencies. Electronic transitions were calculated within the framework of the Time-Dependent DFT [30,31] using the hybrid functional mentioned above. Solvent effects (ethanol) were included implicitly through the Conductor-like Polarizable Continuum Model [32,33]. In order to identify potential coordination sites, charges derived from the molecular electrostatic potential were obtained. MEP-derived atomic charges were calculated according to the scheme proposed by Merz, Singh and Kollman [34]. All the calculations were performed with the Gaussian 09 package [35] and the corresponding figures drawn with Avogadro [36].

It is important to emphasize here that no water molecules were included during the conformational searching or geometry optimizations. This is due to the fact that crystallographic studies show

that water molecules are involved in hydrogen bonds between neighboring molecules in the solid, see below. Present calculations, on the other hand, are carried out on a single molecule in the gas phase, further stabilized by the inclusion of a continuum solvation model.

## Results and discussion

### Crystallographic structural data

#### (HvananS)<sub>2</sub>

There are two closely related independent molecules per crystallographic asymmetric unit. The *rms* separation between homologous non-H atoms in the best least-squares structural fitting, calculated by the Kabsh's procedure [37], is 0.207 Å. Fig. 1 is an ORTEP [38] drawing of one independent molecule.

Each molecule results from the dimerization of 3-methoxy-salicylidene-2-aminothiophenyl monomers through the formation of a disulfide single bond [ $r$  (S1–S2) = 2.030(1) Å and  $r$  (S3–S4) = 2.028(1) Å] with torsion C11–S1–S2–C21 and C31–S3–S4–C41 angles of –81.6(2)° and –83.9(2)°.

All 3-methoxy-salicylideneamino molecular fragments are nearly planar [*rms* deviation of atoms from the best least-squares plane from 0.010 to 0.047 Å], a conformation further stabilized by strong intra-molecular O–H···N bonds [O···N distances from 2.609 to 2.650 Å and O–H···N angles in the 145.2–156.2° range]. As expected, all thiophenyl complementary fragments in the dimers are planar [*rms* deviation of atoms from the best least-squares plane from 0.005 to 0.021 Å]. The monomers within each dimer show significant conformational differences with each other arising from variations in the tilt angle between the 3-methoxy-salicylideneamino and thiophenyl fragments around the corresponding N(i1)–C(i6) ( $i = 1$  to 4)  $\sigma$ -bond linking them. In fact, one monomer shows nearly coplanar fragments [angled at 8.7(2)° and 3.1(2)° from each other for monomers 1 and 3 on different dimers], a conformation favored by intra-molecular O–H···S bonds [ $r$  (O11···S1) = 3.493 Å,  $\angle$ (O11–H···S1) = 132.08° for one dimer and  $r$  (O31–S3) = 3.388 Å,  $\angle$ (O31–H···S3) = 132.27° for the other one]. In the other monomer on each dimer (monomers 2 and 4) the above fragments depart appreciably from co-planarity. In fact, they subtend dihedral angles of 21.8(2)° and 30.2(1)° with each other, conformations that weaken the corresponding intra-molecular O–H···S interactions.

#### (HvananS)<sub>2</sub>·H<sub>2</sub>O

The molecule conformation is closely related to the one found in the anhydrous form. In fact, the *rms* distance between homologous atoms in the best least-squares fitting is less than 0.82 Å. Particularly, within experimental accuracy, the disulfide S–S bond length [2.027(1) Å] is equal and the torsion C11–S1–S2–C21 angle [–86.3(2)°] is close to the values found for the anhydrate. Again, the thiophenyl fragments are planar [*rms* deviations of atoms from the corresponding planes less than 0.021 Å] and both 3-methoxy-salicylideneamino molecular fragments are nearly planar [*rms* deviation of atoms from the best least-squares plane of 0.0722 Å and 0.0307 Å] and stabilized by strong intra-molecular O–H···N bonds [O···N distances of 2.614 Å and 2.660 Å and corresponding O–H···N angles of 145.9° and 144.8°]. In contrast, both monomers show their corresponding 3-methoxy-salicylideneamino and thiophenyl fragments departing significantly from co-planarity. In fact, they subtend dihedral angles of 18.84(8)° (monomer 1) and 34.73(9)° (monomer 2) from each other. As a consequence, the intra-molecular O–H···S bonds are weaker [the strongest one with  $r$  (O11···S1) = 3.513 Å,  $\angle$ (O11–H···S1) = 142.4°] than the corresponding ones found in the anhydrous.

The solid is further stabilized by O11···H–Ow–H···O22' bonds [ $r$  (Ow···O11) = 3.095 Å,  $\angle$ (Ow–H···O11) = 162.6° and  $r$  (Ow···O22') = 3.131 Å,  $\angle$ (Ow–H···O22') = 164.7°] that bridge neighboring molecules giving rise to a polymeric supra-molecular arrangement in the lattice. Fig. 2 is a view of (HvananS)<sub>2</sub>·H<sub>2</sub>O crystal packing showing hydrogen bonding interactions.

### Conformational analysis and geometry optimization

The exploration of the conformational space and optimized geometries, determined both in the gas phase and including solvent effects using DFT tools, provided twenty different conformers. Geometries optimized from X-ray structures with solvent effects were found to be the lowest-energy structures. On the other hand, the conformers obtained through the variation of torsion angles lie more than 7 kcal/mol above in energy. This difference in energy suggests that the conformations obtained from the X-ray structures are the dominant ones. Table 2 shows experimental and calculated values for some relevant geometrical parameters. Complete geometrical data is available as Supplementary material (Tables S1 and S2). It is seen from Table 2 that calculated geometrical parameters are in very good agreement with those parameters found experimentally. The exception is found in O–S distances, for which the calculated values are more than 0.3 Å larger than the experimental ones. This is in accordance with the additional stabilization given by intra-molecular bonds found in the crystal packing (see above). Also, formation of intra-molecular H bonds can be predicted from the calculated structure. Geometrical parameters of the crystal structures of the compounds reported here are in excellent agreement with those found for the crystals obtained from the condensation of 2-aminothiophenol with 5-methoxy-salicylaldehyde [17] and with salicylaldehyde [4].

### MEP-derived atomic charges

MEP-derived atomic charges can be used as a guide to predict potential sites for nucleophilic or electrophilic attacks. With the aim of identifying potential sites for coordination with metals, MEP-derived atomic charges of (HvananS)<sub>2</sub> were calculated. Selected values are listed in Table 3. As it can be seen from the table, oxygen atoms from the OH groups and nitrogen atoms are good candidates to undergo electrophilic attacks as they bear the more negative MEP-derived atomic charges. On the other hand, both oxygen atoms from the OCH<sub>3</sub> groups and sulfur atoms present lower MEP-derived atomic charges than nitrogen atoms and oxygen atoms from OH groups. It can be inferred that this susceptibility would be enhanced after deprotonation of the OH group. It seems then reasonable to propose oxygen atoms belonging to OH groups and nitrogen atoms as potential coordination sites for metal ions.

### Vibrational spectroscopy

The vibrational properties of the solids were examined by infrared and Raman spectroscopies. As expected, the spectra of both compounds were coincident, with the exception of the characteristic bands due to the presence of water in the hydrate. In particular, the bands related to the asymmetric and symmetric H<sub>2</sub>O stretching appear at 3613 and 3535 cm<sup>–1</sup>, respectively, in the spectrum of (HvananS)<sub>2</sub>·H<sub>2</sub>O. The complete assignments of the spectra were done based on reported data [4,8,13,21,39] and with the aid of calculated normal mode frequencies of the gas phase structure. The experimental and calculated values along with the proposed assignment are presented in Table 4 and compared with the data of AT [39] and o-HVa [21] IR spectra. Fig. 3 shows the experimental IR and Raman spectra in the more relevant spectral range, namely 1800–400 cm<sup>–1</sup>.

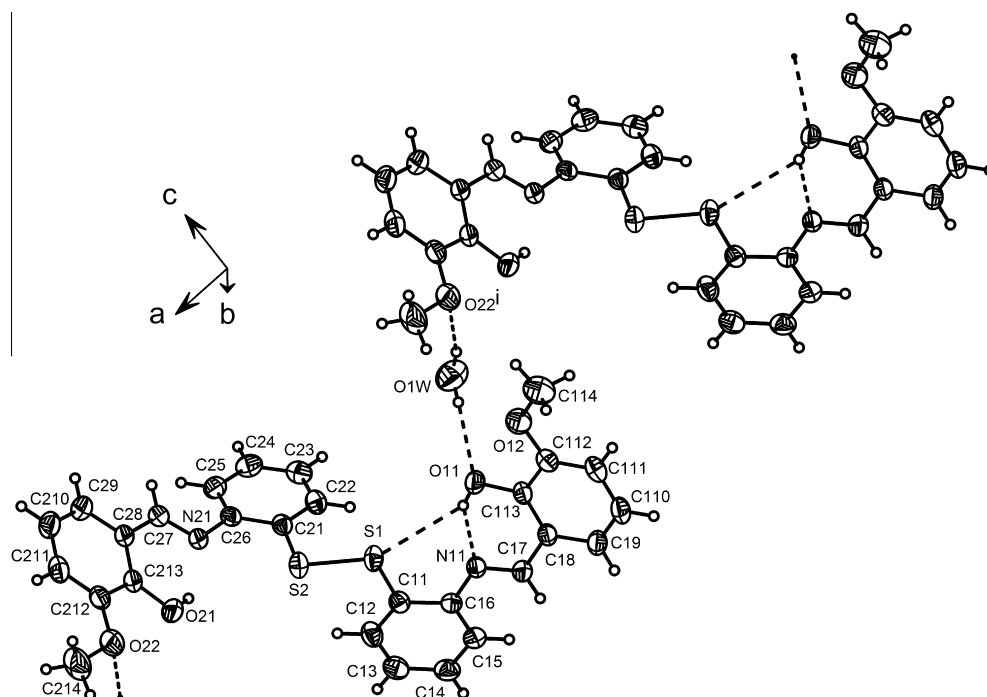


**Fig. 2.** Crystal packing of (HvananS)<sub>2</sub>·H<sub>2</sub>O showing the intra- and inter-molecular hydrogen bonding interactions (in dashed lines). H-bonded neighboring molecules are related through the crystal C-centering symmetry operation (i)  $-0.5 + x, -0.5 + y, z$ .

**Table 2**

Experimental (Exp. 1 and Exp. 2) and calculated selected geometrical parameters for (HvananS)<sub>2</sub>. Atom labels correspond to the ones shown in Fig. 1. Exp. 1. and Exp. 2 are the corresponding conformers found experimentally. d are dihedral angles, in °, and r are distances, in Å. X is either 1 or 3 and Y is either 2 or 4, depending on the conformer, see Fig. 1.

	Exp. 1	Exp. 2	Calc.
d(CY1, SY, SX, CX1)	-81.6	-83.9	-87.7
d(SY, SX, CX1, CX6)	-178.3	-173.1	-169.3
d(CX6, NX1, CX7, CX8)	178.4	178.2	-176.4
d(NX1, CX7, CX8, CX9)	-179.7	177.4	-179.7
d(SX, SY, CY1, CY6)	-169.9	-170.5	-169.3
d(CY6, NY1, CY7, CY8)	-178.8	-177.7	-176.4
d(NY1, CY7, CY8, CY9)	178.1	179.5	179.7
r (S—S)	2.03	2.028	2.059
r OX1—NX1	2.636	2.609	2.621
r OX1—SX	3.493	3.388	3.82
r OY1—NY1	2.65	2.626	2.621

**Table 3**

Negative MEP-derived atomic charges, in units of |e| for (HvananS)<sub>2</sub>.

N11	-0.44
N21	-0.46
O11	-0.63
O12	-0.22
O21	-0.64
O22	-0.22
S1	-0.05
S2	-0.06

Calculations show a strong coupling between several modes. The assignments were done taking into account the predominant modes at each frequency. The IR spectrum of (HvananS)<sub>2</sub> showed a strong band at 1610 cm<sup>-1</sup>, characteristic of the C=N stretching. The modes  $\delta_{as}NH_2$  (1089 cm<sup>-1</sup>),  $\nu SH$  (2524 cm<sup>-1</sup>) and  $\delta SH$

(911 cm<sup>-1</sup>) on AT IR spectrum are absent in (HvananS)<sub>2</sub>. The band attributed to  $\nu C=O$  mode at 1645 cm<sup>-1</sup> in the *o*-HVA spectrum also disappears upon the base formation. Moreover, a band assigned to  $\nu S-S$  at 585 cm<sup>-1</sup> is found, in agreement with the disulfide bond described in the crystal structure.

A review of related literature on the subject reveals discrepancy in the assignments of modes involving sulfur [4,8–10,15,16,18,19]. Generally, infrared spectroscopy data is mentioned in these previous works as a mere characterization tool, without a detailed analysis. Although the synthesis of (HvananS)<sub>2</sub> was similar to the one reported by Soliman et al. [8–10], these authors claim to have obtained a monomer, namely 3-methoxy-salicylidene-2-aminothiophenol. Nevertheless, neither the complete IR spectrum nor the crystal structure has been published by these authors.

#### Electronic spectroscopy

The electronic spectra of ethanolic solutions ( $3 \times 10^{-5}$  M) of the two compounds were registered in the 200–800 nm spectral range. As expected, both spectra were coincident. For the sake of simplicity, only results for the anhydrous (HvananS)<sub>2</sub> are shown. Both experimental and calculated electronic spectra of (HvananS)<sub>2</sub> are depicted in Fig. 4. In Table 5 experimental absorption bands and calculated electronic transitions are listed, together with the proposed assignments. The assignments were accomplished on the basis of calculated electronic transitions and with the aid of reported data for similar compounds [4,7,10].

The spectrum shows a strong absorption between 200 and 350 nm, with two well defined maxima at 204 nm and 222 nm. A series of less resolved bands are observed between 268 nm and 346 nm.

Calculations show that many-body effects are far from negligible for (HvananS)<sub>2</sub>, a fact that is reflected in that most transitions are described by two or more one-electron excitations, involving several MO's. Thus for simplicity only the dominant transitions, chosen according to their oscillator strength, are used to assign the observed bands. It can be seen from Table 5 that the calculated

**Table 4**  
Complete assignment of the IR and RAMAN spectra of (HvananS)<sub>2</sub>. Experimental data of AT and *o*-HVA are included for comparison. Frequencies are given in cm<sup>-1</sup>. Modes indicated with \* are only present in (HvananS)<sub>2</sub>·H<sub>2</sub>O.

AT <sup>a</sup>		<i>o</i> -HVA <sup>b</sup>		(HvananS) <sub>2</sub>		Calculated	Assignments
IR	Raman	IR	Raman	IR	Raman		
				3616 <sup>*</sup> m			v <sub>as</sub> H <sub>2</sub> O
				3534 <sup>*</sup> w			v <sub>s</sub> H <sub>2</sub> O
3449 vs	3432 w						v <sub>as</sub> NH <sub>2</sub>
3357 vs	3358 w						v <sub>as</sub> NH <sub>2</sub>
		3088 vw	3083 vw		3081 vw	3221	vCH( <i>o</i> -HVA)ip
		3069 vw	3073 vw			3228	vCH( <i>o</i> -HVA)op
3064 m	3068 s					3201	vCH
	3050 vs						vCH
		3039 vw	3041 vw	3052 vw		3093	v <sub>as</sub> CH(methyl)
3018 m	3022 m						vCH
		3014 w	3016 w	3012 vw		3303	vOH
		2973 w	2976 vw				v <sub>as</sub> CH(methyl)
		2939 w	2942 vw	2939 vw		3067	vCH(aldehyde)
		2884 w	2887 vw	2838 vw	2840 vw	3026	v <sub>s</sub> CH(methyl)
		2839 w	2849 vw				vCH(aldehyde)
2524 m	2532 m						vSH
		1645 vs	1641 s				vC=O( <i>o</i> -HVA)
1610 vs	1610 m						δ <sub>s</sub> NH <sub>2</sub>
1585 sh	1586 vw	1591 sh	1589 w	1610 s	1612 vs	1696	vC=N + vC-C ring
1574 sh	1572 w			1567 m	1568 s	1642	vring + v <sub>ip</sub> C-OCH <sub>3</sub> + vC=N-C
1481 vs	1480 vw						
1448 vs	1448 vw						
		1471 m	1470 m	1487 sh	1490 w	1524	δ <sub>as</sub> CH <sub>3</sub>
		1455 s	1458 m	1459 s	1459 m	1517	δ <sub>s</sub> CH <sub>3</sub>
					1445 sh	1507	δCH ring
		1388 s		1389 m	1393 vw	1394	δOH <sub>ip</sub> + δCH ring + δCH aldehyde
				1370 sh	1371 vw	1393	δOH <sub>op</sub> + δCH ring + δCH aldehyde
		1327 s	1330 s	1330 w	1335 w	1342	vAr-OH
1307 vs	1306 m			1276 m	1288 w	1315	vC-N (AT) + v <sub>op</sub> C-OCH <sub>3</sub>
					1272 w		
		1257 s	1275 vw	1252 vs	1253 vw	1303	δCH(ring + aldehyde)
					1234 w	1273	
1251 m	1258 m-w	1217 m	1218 m				(vC-C + δCH)aldehyde + δCHring
		1184 sh	1187 vw				δCH + ρO-C-H (methyl)
		1163 m-w		1194 m	1196 m	1224	ρ <sub>r</sub> CH <sub>3</sub>
1159 s	1162 s			1169 sh	1169 w	1201	δCH
1142 m	1144 w			1128 sh	1159 sh	1185	
					1134 vw		
1089 m	1084 w						δ <sub>as</sub> NH <sub>2</sub>
		1070 s	1092 w	1080 w	1082 vw	1152	vC-O(OCH <sub>3</sub> ) + δOH + δCH( <i>o</i> -HVA)
1049 w	1052 w			1055 sh		1087	δ <sub>ring</sub> + δCH
1026 s	1028 w			1035 w	1040 w	1070	δ <sub>ring</sub> + vCS
		947 s	946 vw	969 m	977 w	1015	δ <sub>ring</sub> + vC-O(O-CH <sub>3</sub> )
969 w	970 vw	895 w		942 sh		1006	γCH aldehyde
963 w	940 w						
911 m	910 m						δSH
832 m	838 m-s			856 w	863 vw	887	δring + δCNC
		838 m	837 w	835 vw	835 vw	814	γOH
		779 w		780 m			δring
		763 s		755 m			γCH ring + aldehyde ( <i>o</i> -HVA)
							γCH ring
850 m							
749 s	754 w	737 m	740 vw				
710 w	718 w						
677 m	680 m-s	717 s	718 m	737 s	737 vw		δring + δCH aldehyde + δ(Ar-OCH <sub>3</sub> )
557 w	564 m			685 sh	685 vw		
534 m	542 w			585 vw	557 vw		
				547mw	538 vw		τCC
				453 w	457 w		vSS
	484 m						vCS
	374 m						δCS
	262 m						γCN
	170 s						γCS

vs: very strong; s: strong; m: medium; w: weak; vw: very weak; b: broad; sh: shoulder; ip: in-phase; op: out-of phase.

<sup>a</sup> Data extracted from Ref. [39].

<sup>b</sup> Data extracted from Ref. [21].

transitions describe very well the experimental electronic spectrum.

HOMO and HOMO-1 are  $\pi$  in character in the *o*-HVA rings and non-bonding in the oxygen atoms of the OH and O-CH<sub>3</sub> groups. HOMO-2 and HOMO-3 are also  $\pi$  in character in the benzene rings

and they are mainly non-bonding in the nitrogen and sulfur atoms. HOMO-4 and HOMO-5 are localized in both *o*-HVA and AT rings, showing a  $\pi$  character. Those MO's exhibit also a non-bonding character in nitrogen and sulfur atoms. LUMO and LUMO + 1 are located in the C=N bonds and in the *o*-HVA ring to a minor extent.

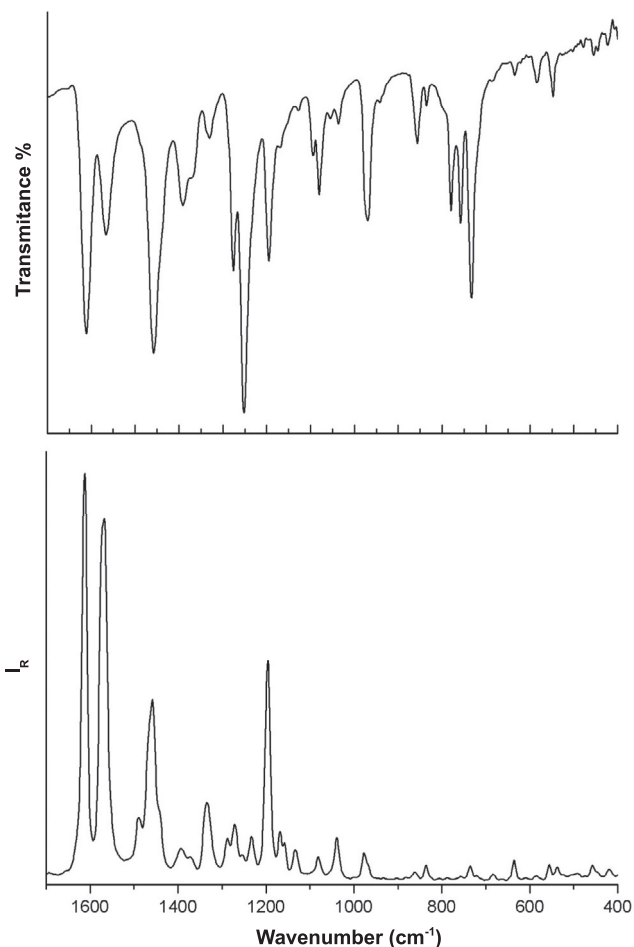


Fig. 3. Experimental IR and Raman spectra of (HvananS)<sub>2</sub> in the 1800–400 cm<sup>-1</sup> spectral range.

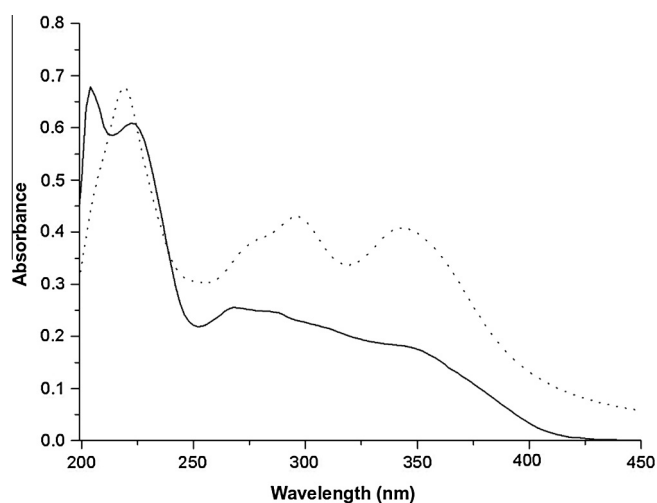


Fig. 4. Electronic spectra of  $3 \times 10^{-5}$  M ethanolic solution of (HvananS)<sub>2</sub>. Experimental (–) and calculated (– –) spectra are shown.

They show a  $\pi^*$  character in the C=N group and a non-bonding character in the *o*-HVa ring. LUMO + 5 and LUMO + 6 present a weak  $\pi^*$  character in the AT rings and they are mainly non-bonding in the nitrogen atoms. LUMO + 7 is mostly localized in *o*-HVa rings, exhibiting a  $\pi^*$  character.

On the basis of the description of the MO's given above, the band at 204 nm can be assigned mainly to a  $\pi \rightarrow \pi^*$  transition, from

Table 5

Electronic spectra of  $3 \times 10^{-5}$  M ethanolic solution of (HvananS)<sub>2</sub>. Calculated electronic transitions for isomer 1 are also shown. Only those calculated electronic transitions relevant for the assignments are listed. Absorption maxima are given in nm. Oscillator strengths of calculated transitions, shown in parenthesis, are in atomic units.

Exp.	Calc.	Assignment
204	205 (0.2336)	HOMO-4 $\rightarrow$ LUMO + 5 (46%)
222	220 (0.5721)	HOMO-2 $\rightarrow$ LUMO + 7 (24%) HOMO $\rightarrow$ LUMO + 6 (35%)
268	278 (0.1871)	HOMO-5 $\rightarrow$ LUMO + 1 (48%) HOMO-4 $\rightarrow$ LUMO (20%)
284	298 (0.4023)	HOMO-5 $\rightarrow$ LUMO + 1 (33%) HOMO-4 $\rightarrow$ LUMO (59%)
306	341 (0.4528)	HOMO-3 $\rightarrow$ LUMO + 1 (51%) HOMO-2 $\rightarrow$ LUMO (46%)
346	361 (0.2123)	HOMO-1 $\rightarrow$ LUMO (47%) HOMO $\rightarrow$ LUMO + 1 (53%)

the *o*-HVa and AT rings to the AT ring. The observed band at 222 nm is assigned to a  $\pi \rightarrow \pi^*$  transition, from the *o*-HVa and AT rings with non-bonding contributions from oxygen, nitrogen and sulfur atoms to the *o*-HVa and AT rings with non-bonding contributions from nitrogen. The broad band between 268 nm and 344 nm is also assigned to a  $\pi \rightarrow \pi^*$  transition, from both aromatic rings to the C=N moiety mainly.

Drawings of the MO's involved in the electronic transitions are depicted in Figs. S1 and S2 of the Supplementary material.

## Conclusions

The condensation reaction of *o*-HVa and 2-aminothiophenol leads to the formation of a disulfide-linked Schiff base. Surprisingly, addition of water to the ethanolic solution of the compound does not produce the hydrolytic decomposition back-reaction, but leads to the formation of the monohydrate compound. Both solids were obtained as single crystals suitable for structural X-ray diffraction study. The molecule conformations are similar to each other, with two closely related independent molecules per crystallographic asymmetric unit. Nevertheless, some significant differences can be observed in each compound. Both solids are further stabilized by intra- and inter-molecular H-bonds.

The calculated geometric features agree very well with the structural parameters derived from crystallographic data. IR and Raman bands, characteristic of the Schiff base formation and of the presence of the S–S bond, were identified. Calculated harmonic frequencies were of assistance to the complete assignment of the experimental vibration spectra. Moreover, theoretical results show a strong coupling between several modes at each calculated frequency.

As expected, the electronic spectra in ethanol of both compounds are coincident and the one of (HvananS)<sub>2</sub> was assigned with the help of calculated data. Most transitions are described by two or more one-electron excitations, involving several molecular orbitals. There is a good agreement between the observed electronic absorption bands and the calculated excitation energies.

MEP-derived atomic charges calculations reveal that the disulfide Schiff base could have several possible coordination sites for metal ions, resulting in a good candidate as a polifunctional quelaing agent.

## Acknowledgments

This work was supported by CONICET (CCT-La Plata), UNLP and ANPCyT, Argentina. V.F.C. is a Post-doctoral Fellow of CONICET. G.A.E., O.E.P., R.P.D. and A.C.G.B. are members of the Research Career of CONICET.

## Appendix A. Supplementary material

Drawings of the occupied and unoccupied molecular orbitals involved in the electronic transitions of (HvananS)<sub>2</sub> are shown in Figs. S1 and S2, respectively. Complete geometrical parameters of both anhydrous and hydrated compounds are listed in Tables S1 and S2, respectively. Fractional coordinates and equivalent isotropic displacement parameters of the non-H atoms for both compounds are shown in Tables S3 and S4, respectively. Atomic anisotropic displacement parameters are presented in Tables S5 and S6 for the compounds under study in the present work. The position of hydrogen atoms and hydrogen bond distances and angles are listed in Tables S7 and S8, respectively.

CIF files with details of the crystal structures reported in the paper are included and have been deposited with the Cambridge Crystallographic Data Center, under deposition number 928403 [(HvananS)<sub>2</sub>] and 928404 [(HvananS)<sub>2</sub>·H<sub>2</sub>O]. Inquiries for data can be directed to: Cambridge Crystallographic Data Centre, 12 Union Road, Cambridge, UK, CB2 1EZ or (e-mail) deposit@ccdc.cam.ac.uk or (fax) +44 (0) 1223 336033. Any request to the Cambridge Crystallographic Data Center for this material should quote the full literature citation and the corresponding reference number.

Supplementary data associated with this article can be found, in the online version, at <http://dx.doi.org/10.1016/j.saa.2013.08.072>.

## References

- [1] A.H. Kianfar, M. Paliz, M. Roushani, M. Shampisur, *Spectrochim. Acta A* 82 (2011) 44–48.
- [2] A.A. Khandar, C. Cardin, S.A. Hosseini-Yazdi, J. McGrady, M. Abedi, S.A. Zarei, Y. Gan, *Inorg. Chim. Acta* 363 (2010) 4080–4087.
- [3] I. Yilmaz, H. Temel, H. Alp, *Polyhedron* 27 (2008) 125–132.
- [4] D. Wang, A. Behrens, M. Farahbakhsh, J. Gätjens, D. Rehder, *Chem. Eur. J.* 9 (2003) 1805–1813.
- [5] A.A. Nejo, G.A. Kolawole, A.O. Nejo, *J. Coord. Chem.* 63 (2010) 4398–4410.
- [6] G.G. Mohamed, M.M. Omar, A.M. Hindy, *Turk. J. Chem.* 30 (2006) 361–382.
- [7] D.A. Chowdhury, M.N. Uddin, F. Hoque, *Chiang Mai J. Sci.* 37 (2010) 443–450.
- [8] A.A. Soliman, W. Linert, *Thermochim. Acta* 338 (1999) 67–75.
- [9] A.A. Soliman, G.G. Mohamed, *Thermochim. Acta* 421 (2004) 151–159.
- [10] A.A. Soliman, *Spectrochim. Acta A* 53 (1997) 509–515.
- [11] K. Sorasaene, J.R. Galán-Mascarós, K.R. Dunbar, *Inorg. Chem.* 41 (2002) 433–436.
- [12] M. Behpour, S.M. Ghoreishi, N. Mohammadi, N. Soltani, M. Salvati-Niasari, *Corros. Sci.* 52 (2010) 4046–4057.
- [13] H. Temel, S. Pasa, Y.S. Ocak, I. Yilmaz, S. Demir, I. Ozdemir, *Synthetic. Met.* 161 (2012) 2765–2775.
- [14] A. Donzelli, I. Metushi, P.G. Potvin, *Inorg. Chem.* 51 (2012) 5138–5145.
- [15] S. Priyarega, R. Prabhakaran, K.R. Aranganayagam, R. Karvembu, N. Natarajan, *Appl. Organometal. Chem.* 21 (2007) 788–793.
- [16] A.A. Soliman, W. Linert, *Monatsh. Chem.* 138 (2007) 175–189.
- [17] C. Ruiz-Pérez, J. González-Platas, F.V. Rodríguez-Romero, P. Gili, P. Martín-Zarza, G. Martín-Reyes, X. Solans, *Acta Crystallogr. C* 51 (1995) 1016–1018.
- [18] A.A. Soliman, *J. Therm. Anal. Calorim.* 63 (2001) 221–231.
- [19] C. Jayabalakrishnan, K. Natarajan, *Transit. Metal. Chem.* 27 (2002) 75–79.
- [20] A. Blagus, D. Cincić, T. Friščić, B. Kaitner, V. Stilinovic, *Maced. J. Chem. Chem. Eng.* 29 (2010) 117–138.
- [21] A.C. González-Baró, R. Pis-Diez, B.S. Parajón-Costa, N.A. Rey, *J. Mol. Struct.* 1007 (2012) 95–101.
- [22] CrysAlisPro, Oxford Diffraction Ltd., version 1.171.33.48 (release 15-09-2009 CrysAlis171.NET).
- [23] G.M. Sheldrick, *SHELXS-97*, Program for Crystal Structure Resolution. Univ. of Göttingen: Göttingen, Germany, 1997 (see also: G.M. Sheldrick, *Acta Crystallogr. A* 46 (1990) 467–473).
- [24] G.M. Sheldrick, *SHELXL-97*, Program for Crystal Structures Analysis. Univ. of Göttingen: Göttingen, Germany, 1997 (see also: G. M. Sheldrick, *Acta Crystallogr. A* 64 (2008) 112–122).
- [25] J.J.P. Stewart, *J. Mol. Modeling* 13 (2007) 1173–1213. MOPAC2012, James J. P. Stewart, *Stewart Computational Chemistry*, Colorado Springs, CO, USA, <http://OpenMOPAC.net>, 2012.
- [26] C. Adamo, V. Barone, *J. Chem. Phys.* 110 (1999) 6158–6170.
- [27] R. Krishnan, J.S. Binkley, R. Seeger, J.A. Pople, *J. Chem. Phys.* 72 (1980) 650–654.
- [28] A.D. McLean, G.S. Chandler, *J. Chem. Phys.* 72 (1980) 5639–5649.
- [29] T. Clark, J. Chandrasekhar, G.W. Spitznagel, P.V.R. Schleyer, *J. Comput. Chem.* 4 (1983) 294–301.
- [30] A. Dreuw, M. Head-Gordon, *Chem. Rev.* 105 (2005) 4009–4037.
- [31] P. Elliott, F. Furche, K. Burke, *Rev. Comp. Chem.* 26 (2009) 91–165.
- [32] V. Barone, M. Cossi, *J. Phys. Chem. A* 102 (1998) 1995–2001.
- [33] M. Cossi, N. Rega, G. Scalmani, V. Barone, *J. Comput. Chem.* 24 (2003) 669–681.
- [34] U.C. Singh, P.A. Kollman, *J. Comput. Chem.* 5 (1984) 129–145; B.H. Besler, K.M. Merz Jr., P.A. Kollman, *J. Comp. Chem.* 11 (1990) 431–439.
- [35] M.J. Frisch, G.W. Trucks, H.B. Schlegel, G.E. Scuseria, M.A. Robb, J.R. Cheeseman, G. Scalmani, V. Barone, B. Mennucci, G.A. Petersson, H. Nakatsuji, M. Caricato, X. Li, H.P. Hratchian, A.F. Izmaylov, J. Bloino, G. Zheng, J.L. Sonnenberg, M. Hada, M. Ehara, K. Toyota, R. Fukuda, J. Hasegawa, M. Ishida, T. Nakajima, Y. Honda, O. Kitao, H. Nakai, T. Vreven, J.A. Montgomery, Jr., J.E. Peralta, F. Ogliaro, M. Bearpark, J.J. Heyd, E. Brothers, K.N. Kudin, V.N. Staroverov, T. Keith, R. Kobayashi, J. Normand, K. Raghavachari, A. Rendell, J.C. Burant, S.S. Iyengar, J. Tomasi, M. Cossi, N. Rega, J.M. Millam, M. Klene, J.E. Knox, J.B. Cross, V. Bakken, C. Adamo, J. Jaramillo, R. Gomperts, R.E. Stratmann, O. Yazyev, A.J. Austin, R. Cammi, C. Pomelli, J.W. Ochterski, R.L. Martin, K. Morokuma, V.G. Zakrzewski, G.A. Voth, P. Salvador, J.J. Dannenberg, S. Dapprich, A.D. Daniels, O. Farkas, J.B. Foresman, J.V. Ortiz, J. Cioslowski, D.J. Fox, *Gaussian 09*, Revision B.01, Gaussian, Inc., Wallingford, CT, 2010.
- [36] M.D. Hanwell, D.E. Curtis, D.C. Lonie, T. Vandermeersch, E. Zurek, G.R. Hutchison, *J. Cheminformatics* 4 (2012) 1–17.
- [37] W. Kabsch, *Acta Crystallogr. A* 32 (1976) 922–923.
- [38] C.K. Johnson, *ORTEP-II*. A Fortran Thermal-Ellipsoid Plot Program. Report ORNL-5318, Oak Ridge National Laboratory, Tennessee, USA, 1976.
- [39] W.P. Griffith, T.Y. Koh, *Spectrochim. Acta A* 51 (1995) 253–267.